X-Ray crystallographic, NMR and antimicrobial activity studies of magnesium complexes of fluoroquinolones – racemic ofloxacin and its S-form, levofloxacin

ARTICLE *in* JOURNAL OF INORGANIC BIOCHEMISTRY · DECEMBER 2006

Impact Factor: 3.44 · DOI: 10.1016/j.jinorgbio.2006.06.011 · Source: PubMed

7 AUTHORS, INCLUDING:

Tormod Skauge
Uni Research AS
15 PUBLICATIONS **149** CITATIONS
SEE PROFILE

Einar Sletten
University of Bergen
107 PUBLICATIONS **1,880** CITATIONS
SEE PROFILE

Kristina Sepcic
University of Ljubljana
125 PUBLICATIONS **2,006** CITATIONS
SEE PROFILE

Available online at www.sciencedirect.com
ScienceDirect
Journal of Inorganic Biochemistry 100 (2006) 1755–1763
Journal of Inorganic Biochemistry
www.elsevier.com/locate/jinorgbio

X-Ray crystallographic, NMR and antimicrobial activity studies of magnesium complexes of fluoroquinolones – racemic ofloxacin and its *S*-form, levofloxacin

Petra Drevenšek [a], Janez Košmrlj [a], Gerald Giester [b], Tormod Skauge [c], Einar Sletten [c], Kristina Sepčić [d], Iztok Turel [a,*]

[a] *Faculty of Chemistry and Chemical Technology, University of Ljubljana, Aškerčeva 5, SI-1000 Ljubljana, Slovenia*
[b] *Institut für Mineralogie und Kristallographie, Geozentrum, Universität Wien, Althanstrasse 14, A-1090 Wien, Austria*
[c] *Department of Chemistry, University of Bergen, Allégaten 41, 5007 Bergen, Norway*
[d] *Biotechnical Faculty, Department of Biology, University of Ljubljana, Večna pot 111, 1000 Ljubljana, Slovenia*

Received 19 June 2006; accepted 25 June 2006
Available online 4 July 2006

Abstract

The magnesium complexes of racemic ofloxacin (oflo) and its pure *S*-form levofloxacin (*S*-oflo) have been studied by X-ray crystallography and NMR spectroscopy. Two compounds, $[Mg(R\text{-oflo})(S\text{-oflo})(H_2O)_2]\cdot 2H_2O$ (**1**) and $[Mg(S\text{-oflo})_2(H_2O)_2]\cdot 2H_2O$ (**2**), respectively, have been prepared by hydrothermal reactions and their crystal structures have been determined. In both structures the anionic fluoroquinolone ligands are coordinated through the keto and carboxylate oxygens forming 1:2 Mg:oflo complexes. The two structures are practically identical except for the orientation of one of the oxazine methyl groups at the chiral center of **2** which was found in equatorial position, the other oxazine methyl groups in **1** and **2** being axial. This difference affects the stacking pattern of quinolone molecules in the cell. ^{1}H NMR chemical shift data and Mn(II) paramagnetic line broadening measurements on the free ofloxacin suggest that the coordination of the ligands in solution involves the keto and carboxylate oxygens. However, it is not possible to decide whether the complexes in aqueous solution have 1:1 or 1:2 stoichiometry. The methylated piperazine nitrogen does not interact with the metal ion. Magnesium–quinolone interaction is discussed in relation to the biological activity of quinolones. The antimicrobial activity of the complexes against various microorganisms was tested and it was established that their activity is similar to that of free quinolone drugs.

Keywords: Antibiotics; Magnesium; X-ray diffraction; NMR spectroscopy; Biological activity

1. Introduction

The research and development of quinolone antibacterial agents have seen an enormous worldwide effort for more than forty years. Over 10,000 structurally related compounds have been isolated and described in patents and scientific papers [1]. Several fluoroquinolones in clinical use feature a carboxyl group at position 3, a keto group at position 4, a fluorine at position 6, and a piperazinyl or methyl piperazinyl group at position C-7. Differences at the moiety present at the N-1 and at the C-7 position markedly influence the microbiological activity and pharmacokinetic properties [2]. The ofloxacin molecule possesses an oxazine ring in which positions C-8 and N-1 are linked via the ring structure (Scheme 1). Attached to this ring is a methyl group that can exist in two optically active forms, the *S*-isomer being up to two orders of magnitude more potent than the *R*-isomer. The phenomenon is surprising, since the difference in structure between the enantiomers is only the steric configuration of a presumably non-functional methyl group relative to the ring plane. Initially, only racemic ofloxacin was available as a drug, but has now largely been replaced by the optical *S*-isomer (*S*-oflo) (trade name

* Corresponding author. Tel.: +386 1 2419124; fax: +386 1 2419220.
E-mail address: iztok.turel@fkkt.uni-lj.si (I. Turel).

0162-0134/$ - see front matter © 2006 Elsevier Inc. All rights reserved.
doi:10.1016/j.jinorgbio.2006.06.011

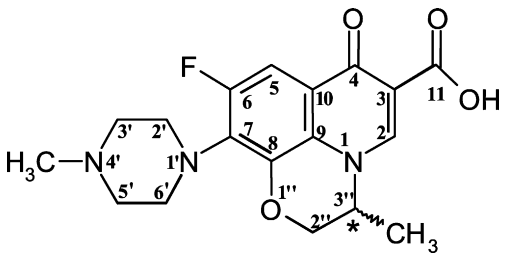

Scheme 1. Formulae of ofloxacin (*R*-, *S*-) or levofloxacin (*S*-) with numbering scheme (∗ denotes the chiral centre).

levofloxacin) which is currently a leader on the quinolone drug market.

There are several families of antibiotics that require metal ions to function properly and were also dubbed "metalloantibiotics" [3]. Metal ions play a key role in the actions of metalloantibiotics and are involved in specific interactions of these antibiotics with various biomolecules (proteins, membranes, nucleic acids and others). Magnesium (as a very common ion in biological systems) is not only important for the activity of quinolones but also for some other antibacterial agents, such as aureolic acid and derivatives, various tetracyclines and some other.

The target of the quinolones is the DNA gyrase, which changes negative superhelical coils into covalent circular DNA [4]. Both enantiomers have been found to bind to calf thymus DNA with higher affinity for the *S*-isomer than the *R*-isomer [5,6]. It is well-known that metal ions coordinate to quinolones, and several complexes have been isolated and characterized [7–9]. Antacids containing magnesium or aluminium markedly impair the absorption of orally administered fluoroquinolones. The decrease in absorption may be as great as tenfold. The mechanisms of action of various quinolones are not fully understood, but many of the theories focus on the involvement of magnesium ions [10–15]. It is not yet known whether the magnesium ion influence is due to its stabilizing effect on DNA topology or its ability to chelate with the keto and carboxylate moieties of quinolones.

Previously we have studied the interactions of magnesium and fluoroquinolones as well as the influence of magnesium on the interaction between fluoroquinolones and DNA oligodeoxyribonucleotides [16–18]. Here we report the crystal structures of $[Mg(R\text{-oflo})(S\text{-oflo})(H_2O)_2]\cdot 2H_2O$ (**1**) and $[Mg(S\text{-oflo})_2(H_2O)_2]\cdot 2H_2O$ (**2**), ^1H NMR spectroscopic solution studies, and antibacterial activity of the corresponding systems.

2. Experimental

2.1. Synthesis

2.1.1. $[Mg(R\text{-oflo})(S\text{-oflo})(H_2O)_2]\cdot 2H_2O$ (1) and $[Mg(S\text{-oflo})_2(H_2O)_2]\cdot 2H_2O$ (2)

Compound **1** was synthesized by a hydrothermal reaction from a mixture of ofloxacin (0.126 g, 0.350 mmol), magnesium chloride hexahydrate (35.6 mg) and L-histidine (27.2 mg) in the molar ratio of 2:1:1. Distilled water (1.0 mL) was added to the mixture of reactants and placed in a tube and pH was adjusted to 7 with 2 M NaOH. The tube was then frozen by liquid nitrogen, evacuated and sealed. The ampoule was heated at 120 °C for 3 days to give pale yellow crystals of **1**. Yield: 8.9%. $C_{36}H_{46}F_2MgN_6O_{12}$: calcd. C 52.92, H 5.67, N 10.29; found: C 52.91, H 5.58, N 10.25. FTIR (cm^{-1}, Nujol; m, medium; w, weak; s, strong): 3367(m), 1683(w), 1616(s), 1580(s), 1292(m), 1274(m), 1230(w), 1201(w), 1154(w), 1133(w), 1116(w), 1094(w), 1050(m), 1008(m), 982(m), 959(w), 940(w), 890(w), 843(w), 818(m), 786(w), 768(w), 747(w), 725(w), 694(w), 654(w), 632(w).

The procedure to prepare **2** was similar with the important difference that this synthesis was successful only in the absence of histidine. The amount of *S*-ofloxacin was 0.500 mmol (0.181 g), and 0.250 mmol (50.8 mg) of magnesium chloride hexahydrate was added. The ampoule was heated at 130 °C for 1 day to give yellow crystals of **2**. Yield: 8.1%. $C_{36}H_{46}F_2MgN_6O_{12}$: calcd. C 52.92, H 5.67, N 10.29; found: C 52.91, H 5.69, N 10.29. FTIR (cm^{-1}, Nujol): 3354(m), 1692(w), 1614(s), 1576(s), 1290(m), 1273(m), 1230(w), 1199(w), 1152(w), 1133(w), 1114(w), 1081(m), 1069(m), 1046(m) 1008(m), 981(m), 959(w), 945(w), 895(w), 842(w), 818(m), 785(w), 766(w), 746(w), 725(w), 686(w), 655(w), 630(w).

Infrared spectra (Nujol) were recorded on a Perkin–Elmer FT-1720X spectrometer. The UV–Visible spectra were recorded on a Perkin–Elmer Lambda 6 UV–Visible spectrophotometer using 500 μL Quartz cuvettes (Hexxa) and pH was measured using a Sentron Argus pH meter equipped with a Sentron ISFET Hotline probe. Elemental analyzes were performed on a Perkin–Elmer 204C microanalyzer. The following chemicals were used: $MgCl_2\cdot 6H_2O$ (Fluka), levofloxacin (Fluka), ofloxacin (Sigma), L-histidine (Kemika, Zagreb). All were of analytical grade and used as supplied.

2.2. Crystallography

Crystal data and refinement parameters of compounds **1** and **2** are listed in Table 1. Intensity data were collected at 200 K for **1** and 150 K for **2**, respectively on Nonius Kappa CCD diffractometers equipped with a cooling device (Oxford Cryosystems, Cryostream Cooler), a Mo anode ($\lambda = 0.71073$ Å) and a graphite monochromator, and the multiscan absorption correction [19] was performed. The structures were solved by direct methods (SHELXS-97) and refined by a full-matrix least-squares procedure based on F^2 (SHELXL-97) [20]. Hydrogen atoms attached to water oxygen atoms were found in difference Fourier maps and were refined freely. All the remaining H atoms were placed at calculated positions and treated using appropriate riding models.

Structure **1** was initially solved in the centrosymmetric space group $P2_1/a$. It was not, however, possible to refine

Table 1
Crystal data and refinement parameters of compounds **1** and **2**

	1	**2**
Formula	$C_{36}H_{46}F_2MgN_6O_{12}$	$C_{36}H_{46}F_2MgN_6O_{12}$
F_w	817.1	817.1
Crystal system	Monoclinic	Monoclinic
Space group	$P2_1$	$P2_1$
a (Å)	11.0244(3)	10.9761(4)
b (Å)	9.6181(2)	9.7345(4)
c (Å)	18.2476(9)	17.9179(8)
β (°)	97.999(3)	98.219(2)
V (Å^3), Z	1916.0(1), 2	1894.8(1), 2
T (K)	200(2)	150(2)
D_{calcd} (g cm^{-3})	1.416	1.432
μ (Mo Kα) (mm^{-1})	0.127	0.129
Crystal size (mm)	$0.20 \times 0.17 \times 0.10$	$0.15 \times 0.10 \times 0.05$
Crystal colour, shape	Yellow prism	Yellow prism
θ range (°)	3.45–26.37	3.45–26.37
Data measured	15,160, 7804	14,536, 7654
unique (R_{int})	(0.0207)	(0.069)
Observed data [$I > 2\sigma(I)$]	6624	5372
No. of parameters	547	547
R[a], wR_2[b] [$I > 2\sigma(I)$]	0.0459, 0.1136	0.0489, 0.0914
R, wR_2 (all data)	0.0565, 0.1206	0.0927, 0.1078
S[c], $(\Delta/\sigma)_{max}$	1.019, 0.001	1.011, 0.001
Max, min peaks (eÅ^{-3})	0.926, −0.388	0.266, −0.237

[a] $R = \Sigma\|F_o|-|F_c\|/\Sigma|F_o|$.
[b] $wR_2 = \{\Sigma[w(F_o^2 - F_c^2)^2]/\Sigma[w(F_o^2)^2]\}^{1/2}$.
[c] $S = \{\Sigma[(F_o^2 - F_c^2)^2]/(n/p)\}^{1/2}$, where n is the number of reflections and p is the total number of parameters refined.

the structure without invoking disorder in the piperazine ring region. In the best model obtained in this space the piperazine atoms were refined as two parts of a disordered group, and the occupancy factors suggested the presence of equal amounts of the two orientations. At the completion of this refinement the *R*-factor was still high (0.09). A closer inspection of the structure factors showed that although *h*0*l* reflections with $h = 2n + 1$ are generally weak, a significant number of these reflections violated the systematic extinction rule of $P2_1/a$. After conversion to the non-centrosymmetric space group $P2_1$, the refinement of the structure proceeded nicely, and with no sign of disorder in the piperazine region. Each asymmetric unit consists of one Mg-$(oflo)_2$ complex unit in which one of the oflo-ligands is in the *R*-form, and the other in the *S*-form. The deviations from centrosymmetry in structure **1** are further discussed in the section on crystal structures. X-ray refinement of the absolute structures resulted in Flack parameters with high standard deviations, as it often does for light atom structures. Nevertheless, in the case of compound **2** where it is known chemically that both chiral centres are in the *S*-form, the X-ray refinement clearly favoured the correct absolute configuration.

2.3. NMR spectroscopy

Proton and carbon NMR spectra were recorded on Bruker DRX Avance 500, Avance 400 and Bruker Avance DPX 300 spectrometers operating at 500 MHz, 400 MHz and 300 MHz for ^{1}H NMR spectroscopy. 1D ^{1}H spectra were recorded typically using 160 transients collected with 32 K data points at 298 K. Additional spectra were recorded at both higher and lower temperatures using 64-512 transients. 2D ^{1}H–^{13}C HSQC spectra were recorded at 298 and 276 K. Typically 2048 complex points were collected in t_1 with 64-512 increments in t_2, where each increment was averaged over 256 transients. All spectra were referenced to the residual HDO resonance at 4.758 ppm at 298 K. NMR samples of the magnesium–quinolone complexes were prepared by dissolving 0.8 mg and 0.6 mg of **1** and **2**, respectively, in 0.8 mL 99.96% D_2O (Cambridge isotopes). The solutions were shaken at room temperature for 3 h and centrifugated. Concentrations of the saturated solutions of complexes **1** and **2** were determined by UV spectroscopy. As the molar extinction coefficients for these complexes are unknown, the molar extinction coefficient for *S*-oflo, $\varepsilon = 23{,}408\ cm^{-1}\ M^{-1}$, was used as reference [21]. This gave an approximate concentration of 0.14 mM and 0.31 mM for **1** and **2**, respectively. The UV spectra were practically identical, confirming the similarity of the two complexes in solution (data not shown). Of each centrifugate 500 μL were transferred to NMR tubes (Wilmad), pH 8.8. As reference solution, 1 mM free *S*-ofloxacin was used (in D_2O, pH 8.8). Mn(II) titration was carried out on a 1 mM *S*-ofloxacin solution using 0.5–20.0 mM $MnCl_2$(Fluka) in aliquots of 2.5–10.0 μL.

2.4. Antimicrobial activity tests

The antibacterial potential of the magnesium complexes of levofloxacin and ofloxacin was assayed using three Gram positive (*Staphylococcus epidermidis*, *Micrococcus luteus*, *Bacillus subtilis*) and five Gram negative (*Salmonella enteritidis*, *Escherichia coli*, *Klebsiella pneumoniae*, *Pseudomonas aeruginosa*, *Enterococcus foecalis*) bacterial strains. All used bacteria were obtained from the local collection at the Department of Biology, University of Ljubljana.

Antimicrobial activities were evaluated using the agar diffusion test, as described earlier [22–24]. For estimation of minimal inhibitory concentration values (MIC), the antibacterial substances were gradually diluted in 50 mM Tris · HCl buffer pH 7.4. Free levofloxacin and ofloxacin, dissolved in the same buffer, were used as reference compounds.

3. Results and discussion

3.1. Syntheses and crystal structures

It was previously reported that the presence of histidine in the preparation of quinolone metal complexes could result in the isolation of new crystalline products which are different from those obtained without using this compound [25]. In the present case histidine had to be added in order to obtain crystals of **1** while **2** crystallized in the absence of histidine. Histidine may serve to fine-tune the protolytic equilibria to reach the correct species distribution for crystallization. At pH 7 both *S*-oflo and *R*-oflo are present predominantly in neutral and zwitterionic forms ($pK_{a1} = 6.0$, $pK_{a2} = 8.2$) [26]. It was established (see above) by UV measurements in solution that the solubility of **2** is slightly higher than that of **1**.

The molecular structure of **2** is shown in Fig. 1. Selected bond distances and angles are collected in Table 2. All bond distances and angles in both compounds are in agreement with corresponding data cited in the literature [7,27,28].

The common features of **1** and **2** are coordination to magnesium through the keto and carboxylate oxygens (Fig. 1, Table 2). Quinolone molecules are in the anionic form. The slightly distorted octahedral coordination of magnesium is completed by two aqua ligands located in axial positions. The Mg–H_2O distances are significantly longer than the equatorial Mg–carboxyl/keto distances. The piperazine nitrogen does not interact with magnesium, probably due to the steric crowding of the methyl group. It is interesting to note that the hydrothermal reaction of quinolone norfloxacin (with non-methylated piperazine) with various metals at pH 7–8 resulted in a 2D square grid of complexes where also *N*-piperazine is coordinated to the metal [29,30].

The aromatic ring systems of quinolone ligands are predominantly planar and piperazine rings are in the normal chair conformation. The main difference between structures **1** and **2** is related to the orientation of the oxazine methyl groups: one of the two oxazine methyl groups in **2** has adopted an equatorial orientation while all the other oxazine methyl groups are located in axial positions. The values of dihedral angles defining the orientation of the axial oxazine methyl group are in the range 76–78° which is significantly less than the average value of 87° calculated for various metal free oxazine derivatives. The dihedral angle for the only methyl group found with equatorial orientation was determined at 20.1°, significantly less than the calculated value of ~32° [31].

Table 2
Selected geometric parameters of complexes **1** and **2** (Å,°)

	1	**2**
Mg–keto (a)	2.041(2)	2.033(2)
Mg–keto (b)	2.039(2)	2.029(2)
Mg–carboxyl (a)	2.032(2)	2.027(2)
Mg–carboxyl (b)	2.038(2)	2.038(3)
Mg–water (a)	2.086(2)	2.092(2)
Mg–water (b)	2.069(2)	2.077(2)
O (c,a)–Mg–O (k,a)	88.08(9)	87.87(10)
O (c,b)–Mg–O (k,a)	92.65(9)	93.42(9)
O (c,a)–Mg–O (k,b)	91.49(9)	91.09(9)
O (c,b)–Mg–O (k,b)	87.79(9)	87.56(9)
O (c,b)–Mg–O (w,i)	89.73(10)	88.88(11)
O (k,a)–Mg–O (w,i)	90.26(10)	88.03(10)
O (c,a)–Mg–O (w,ii)	89.97(10)	91.38(10)
O (k,a)–Mg–O (w,ii)	89.37(10)	90.95(10)
O (w,i)–Mg–O (w,ii)	179.52(14)	178.94(13)

k = keto; c = carboxyl; w = water.

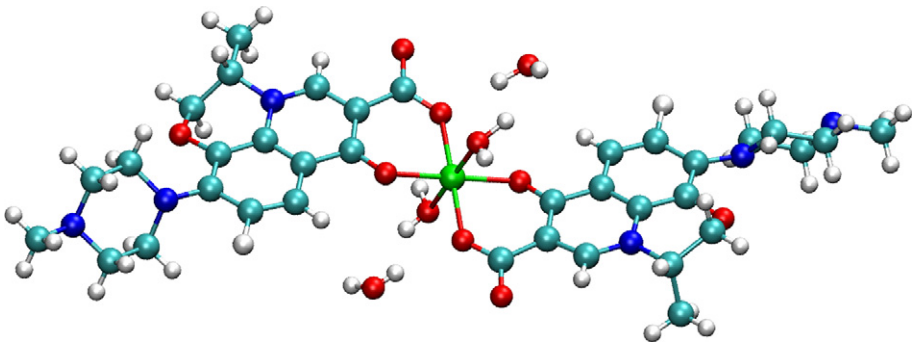

Fig. 1. The molecular structure of **2**. The structure of **1** is practically superimposable except for the orientation of the oxazine methyl group (see below).

The crystal packing arrangements are as expected quite similar for **1** and **2** (Fig. 2). The end-on view of the complexes (Fig. 2a) reveals that the quinolone planes are displaced to opposite sides of the equatorial coordination plane, and in addition there is a distinct propeller twist relative to this plane. Layers of overlapping quinolone rings are stabilized by weak π-π interactions (Fig. 2b). One feature that should be mentioned is that in **1** the perpendicular distance between layers is 4.32(7) Å, whereas in **2** this distance is significantly shorter (4.13(4) Å). This difference, which is due to the respective position of the oxazine methyl group in the two structures, may be important with regards to the ability of **1**and **2** to form stacked aggregates in solution.

Compound **1**, containing (*R*-oflo)(*S*-oflo) groups, was expected to crystallize in a centrosymmetric space group. However, in the course of the refinement (see crystallographic section) it became clear that the orientations of the two piperazine rings break this symmetry. The dihedral angle between best least-squares planes defined by the four carbon atoms of each ring is 89.1° (as opposed to 0° if Mg was positioned at a center of symmetry). This is practically identical to the corresponding dihedral angle found in **2** (89.9°). As described above, the crystal packing in both compounds is quite similar, with overlap between the two different parts of screw axis related molecules (Fig. 2). The relative rotations of the piperazine rings seem to favour a denser packing; the deviation from centrosymmetry may hence be caused by packing effects.

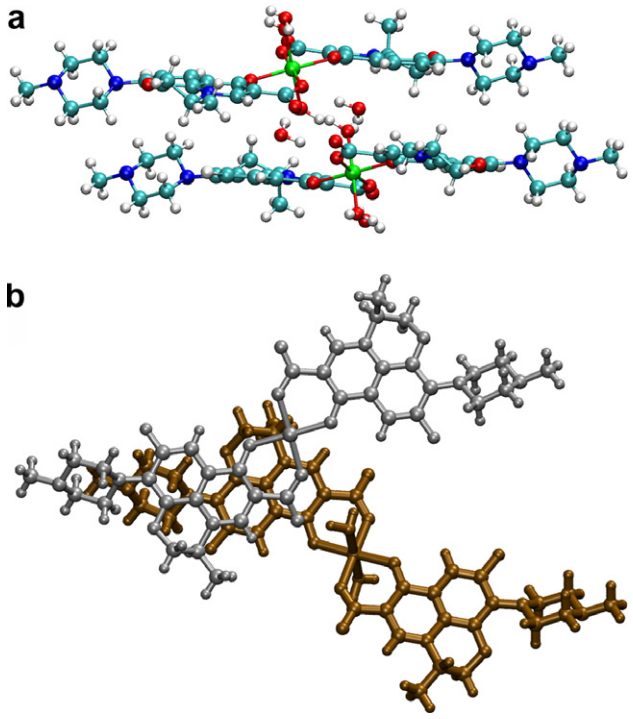

Fig. 2. Crystal packing for **2**. Two complexes are present in each cell. Views parallel and perpendicular to the molecular plane.

3.2. NMR solution studies

The magnesium–quinolone complexes were studied by ^{1}H NMR and compared with the spectra of free quinolones. The solubility of the complexes around physiological pH was too low to obtain proton NMR spectra with sufficient signal-to-noise ratio. The spectra of free quinolones and the complexes **1** and **2** (Fig. 3) exhibit the characteristic features of fluoroquinolone with two aromatic resonances around 7–8.5 ppm, the oxazine resonances close to the water resonance at 4–5 ppm, the piperazine resonances at 2.5–4 ppm, and at approximately 1.5 ppm the oxazine methyl resonance. The proton assignment was checked by 2D ^{1}H–^{13}C HSQC and HMBC experiments (data not shown) and is in agreement with previous work [17,32,33]. However, it was not possible to distinguish between H2″a and H2″b (Scheme 1) resonances and so far no reports have been given with an unambiguous assignment of these signals.

Shimada et al. [34] reported $\log K_1 = 2.82$ for 1:1 magnesium–ofloxacin complex formation, and $\log K_2 = 2.66$ for 1:2 complex formation. Therefore major species present in aqueous solutions of **1** and **2** are expected to be free quinolone, Mg^{2+}(aq) ions and Mg:quinolone complexes (1:2, 1:1). The appearance of only one set of resonances in the NMR spectra of the solutions indicates that the exchange between the species is fast on the NMR timescale.

3.2.1. Chemical shifts

The aromatic resonances show only small chemical shift variations between the magnesium–quinolone complexes and the free quinolones. In other studies [17,35] H2 exhibits a characteristic 0.3–0.5 ppm downfield shift upon binding of a divalent metal ion. The small H2 shift observed may be caused by metal-induced stacking, and this shift could be cancelled by an opposite upfield ring current shift which is expected in stacked aromatic quinolones. The result would be a very small net shift, as observed in the spectra.

3.2.2. Line broadening

The most pronounced differences in the NMR spectra between free *S*-ofloxacin and **1** and **2** are the substantial selective line broadening experienced by H2 and H5 in the complexes (Table 3). The inaccuracy of the measurements of line widths at half-height is relatively large due to low signal-to-noise ratio in the spectra. Line broadening of proton signals may be induced by neighbouring paramagnetic metal centres, quadrupolar effects, proton exchange phenomena or decreased tumbling rate due to aggregate formation. Proton exchange and decreased tumbling rate are excluded on the basis that these effects should be observed for all resonances in the complex. Magnesium(II) as diamagnetic nuclei is not expected to produce paramagnetic line broadening. However, the natural abundance of the quadrupolar ^{25}Mg isotope, spin 5/2 is ~10%, and at stoichiometric ratio this could lead to quadrupolar relaxation of adjacent protons.

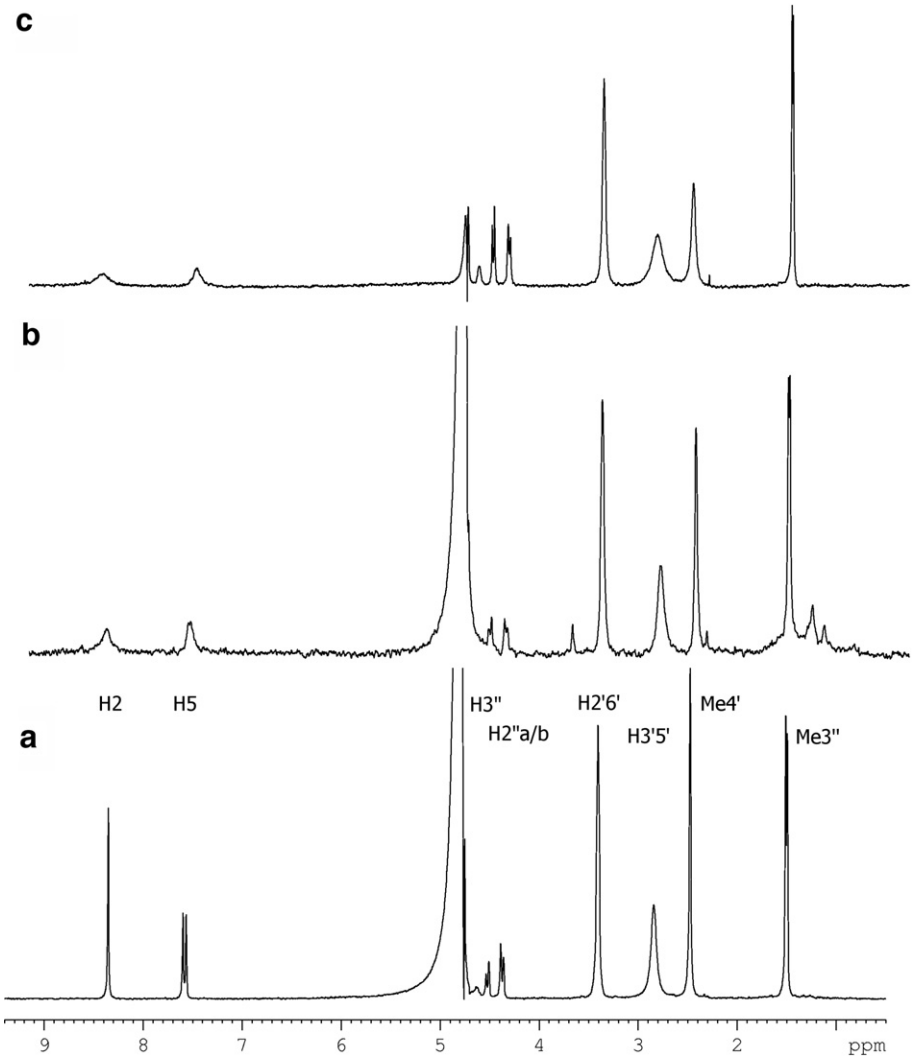

Fig. 3. ^{1}H NMR spectra of *S*-ofloxacin (a), complex **1** (b), and complex **2** (c) at 298 K, pH 8.8. All spectra are referenced to the residual HDO resonance at 4.758 ppm.

The keto and carboxylate oxygen atoms have previously been identified as the metal ion binding site in 1:1 metal/quinolone complexes by NMR and IR spectroscopy [36]. In order to verify that the binding pattern for complexes **1** and **2** are similar to that of 1:1 complexes, Mn(II) was used as a paramagnetic probe assuming that the two metals have similar coordination geometry. Titration of *S*-ofloxacin was carried out by adding aliquots of $MnCl_2$ solution (Figure S1 in Supplementary Material) [37,38]. The line broadening effect is substantial and only sub-stoichiometric concentration of paramagnetic metal ions was needed to detect interaction. The paramagnetic induced line broadening is seen to be significantly larger for H5 than for H2 (Fig. 4, Tables S1 and S2 in Supplementary Material). This is also in agreement with Cu(II) titration data of fluoroquinolones [39]. Assuming that the Mn(II) and Mg(II) positions are about equal the difference in line broadening between H2 and H5 agrees qualitatively with the averaged calculated distances in the two crystal structures (Mg(II)–H2 = 5.2 Å; Mg(II)–H5 = 4.3 Å). The effect of paramagnetic induced line broadening is proportional to r^6, r being the distance between the metal centre and the proton.

The selective line broadening observed for **1** and **2** is consistent with that expected for keto/carboxyl chelation. However, the relative H2/H5 broadening is seen to be opposite of that observed with paramagnetic probes (Table 3). It is difficult to relate this discrepancy to differences in coordination chemistry between Mn(II) and Mg(II).

Lecomte and Chenon [40] hypothesised from ^{19}F NMR spectra of the fluoroquinolone pefloxacin that cation binding occurs first at the methylated piperazine nitrogen N4′ and secondly at the keto and carboxyl oxygen atoms. This would be surprising for ofloxacin, taking into account the pK_a values ($pK_{a1} = 6.0$, $pK_{a2} = 8.2$) and is refuted by the absence of line broadening of the piperazine resonances even at high [Mn(II)]/[ofloxacin] ratios. Sakai et al. [41] have carried out extensive metal binding studies on several fluoroquinolones, however, most of the experiments were performed at pH 2.5, and thus not directly comparable to the present work.

Table 3
^{1}H NMR chemical shifts and line widths of the free quinolones and their magnesium complexes

	Chemical shifts [ppm]		Line widths [Hz]	
	1	**2**	**1**	**2**
H2	8.41	8.43	42.6	82.9
	(0.06)	(0.08)	(38.5)	(78.7)
H5	7.56	7.49	27.0	46.8
	(−0.02)	(−0.09)	(22.8)	(42.5)
H3″	n.a.	4.63	n.a.	18.6
	(n.a.)	(0.00)	(n.a.)	(n.a)
H2″a/	4.53	4.50	7.9	5.5
H2″b	(0.00)	(−0.02)	(1.2)	(−0.1)
H2″b/	4.37	4.34	7.6	7.8
H2″a	(−0.01)	(−0.03)	(0.1)	(2.1)
H2′6′	3.40	3.38	12.4	16.1
	(−0.06)	(−0.02)	(1.5)	(5.0)
H3′5′	2.81	2.84	26.2	63.8
	(−0.22)	(0.00)	(−1.4)	(39.4)
Me4′	2.45	2.47	9.9	23.9
	(−0.18)	(0.00)	(1.5)	(17.5)
Me3″	1.51	1.47	6.5	5.2
	(0.01)	(−0.03)	(2.0)	(0.7)

Differences between free and bound fluoroquinolone given in parenthesis. All shifts are referenced to the residual HDO peak at 4.758 ppm, 298 K. Lines too broad to be measured are designated n.a.

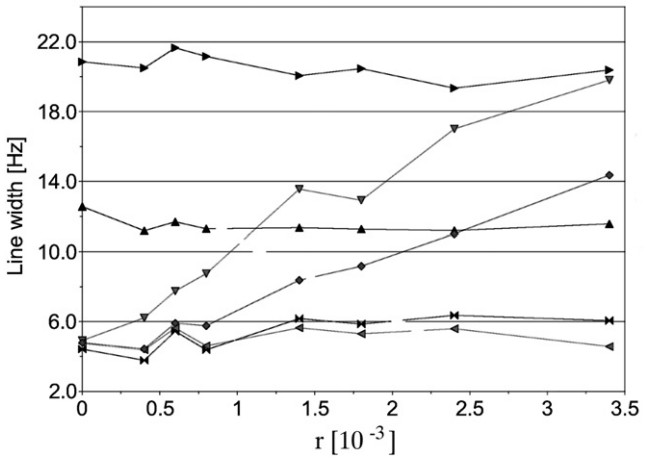

Fig. 4. Plot showing the measured line width of the ^{1}H resonances of *S*-ofloxacin with increasing concentration of Mn(II). The ratio ***r*** is given as [Mn(II):*S*-oflo] (times 10^3): (◆) H2, (▼) H5, (▲) H2′6′, (►) H3′5′, (◄) Me4′, (►◄) Me3″.

The piperazine resonances of the magnesium–quinolone complexes are severely broadened compared to the free quinolones, as seen in Table 3. The largest effect is on the H3′5′and Me4′ resonances, while the H2′6′ show negligible broadening. The H3′5′ resonances are broad also for the free quinolones due to restricted motion of the piperazine ring, ring inversion and/or slow nitrogen-inversion at the deprotonated N4′ site. For deprotonated *N*-methyl piperidines, the methyl group favours equatorial position [42], but the free energy difference for equatorial and axial conformation is very low, ca. 2.7 kcal/mol [43] with an anticipated coalescence temperature of 123 K [44]. The induced broadening of the N4′-methyl resonance can therefore only be attributed to a reduced rate of nitrogen pyramidal inversion if there is a direct or indirect interaction to the N4′ site, e.g. through the first or second hydration sphere. This is not the case as even high ratios of Mn(II)/ofloxacin do not show interactions at the N4′ site. The induced broadening may therefore be ascribed to the metal induced aggregation.

We would like to note that also NMR experiments involving titration of a DNA oligonucleotide with complex **1** and **2** have been carried out. However, due to low solubility in water at physiological pH the sensitivity was not high enough to observe any significant effect on the DNA proton signals.

3.3. Antimicrobial activity tests and biological relevance of magnesium complexes

The susceptibility of bacteria against tested antibiotics is presented in Table 4. As already reported [45,46], levofloxacin exerts higher antibacterial activity than ofloxacin. The same trend was observed with magnesium complexes of both antibiotics.

MIC values of **1** and **2** did not significantly differ from those of the non-complexed compounds, showing a general slight decrease in their antibacterial potential. None of the tested compounds showed any special preference for Gram positive or Gram negative bacterial strains. These results are in agreement with results obtained in our previous studies [22–24,47,48]. Similar antimicrobial activities of metal complexes and free ligands, as observed in most studies of metal-quinolone complexes are not surprising and are probably due to the intracellular biological conversion of the complexes.

The facts that millimolar concentration of magnesium ion is required for tight binding of quinolones to DNA [49] and that also the interaction between gyrase A and quinolones is enhanced in the presence of magnesium [50] suggest that the interactions between magnesium and quinolone are important for drug activity. The intracellular

Table 4
Antibacterial activity of oflo, **1**, *S*-oflo, and **2**

Microorganism	MIC (***μg/ml***)			
	oflo	**1**	*S*-oflo	**2**
Gram positive				
Staphylococcus epidermidis	0.75	1	0.3	0.6
Bacillus subtilis	0.5	0.8	0.3	0.5
Micrococcus luteus	12	20	7	10
Gram negative				
Klebsiella pneumoniae	0.7	1	0.25	0.5
Escherichia coli	0.2	0.25	0.15	0.15
Salmonella enteriditis	0.75	1	0.5	0.75
Pseudomonas aeruginosa	7	10	3	5
Enterococcus faecalis	10	15	4	4

The activity is expressed as MIC (minimal inhibitory concentration, which is the lowest concentration of an antibiotic that will inhibit the growth of a tested organism).

concentration of magnesium ions is much higher than that of quinolone [1,36]. According to the stability constants [34] (see NMR discussion) it can be assumed that also in biological systems the mixture of 1:1 and 1:2 magnesium–quinolone complexes, free quinolones, and hydrated magnesium ions are present. It is probable that magnesium–quinolone complexes and not free quinolones interact with their target DNA–gyrase complex [36,49,51]. On the other hand it is also known that high concentration of extracellular magnesium could antagonize the penetration of fluoroquinolones into the bacterial cell [1].

Magnesium complexes **1** and **2** are not promising as new drugs but are very interesting for their possible role in the mechanism of action of these drugs. Experimental DNA binding data and computer modeling have shown that four *S*-oflo but only two *R*-oflo molecules can fit the proposed DNA binding site [5]. Evidently, a subtle difference in steric configuration of a nonfunctional group causes a dramatic change in affinity for the receptor site. The computer modeling shows that fitting the enantiomers to DNA is critically dependent on the position of the methyl group at the chiral centre. As realized from the crystal structures the distances between the layers of quinolone rings in **2** are shorter than in **1** and this could be relevant for the number of *S*- and *R*-quinolone molecules bonded at the DNA binding site.

We have found some analogies between our complexes and the magnesium complex of aureolic family drug (chromomycin) and it is appealing to propose that the binding of our complexes to DNA could be similar to the binding of magnesium chromomycin complex [3,52]. Two chromomycin ligands are coordinated to magnesium through oxygen atoms and octahedral coordination of the metal is completed by two aqua ligands, which is very similar to our complexes **1** and **2**. The crystal structure shows that magnesium complex of chromomycin binds to GGCC sequence of the octamer's minor groove. Moreover, the authors have also realized that the stacking of the ligand molecules was more intense in the presence of DNA [52]. Unfortunately our attempts to prepare appropriate crystals and to determine the crystal structure of the magnesium–quinolone complex with DNA were not successful so far.

4. Conclusions

The stereochemistry of fluoroquinolones is a key factor for the interaction with DNA and gyrase enzymes and the crystal structures of magnesium complexes of ofloxacin enantiomers show that the conformation of the oxazine methyl group influences the crystal packing. In solution, Mg(II) is bound to the keto-carboxylate oxygen atoms, but not to the terminal piperazine nitrogen as shown by Mn(II) titration. The ^{1}H NMR spectra of the solutions containing **1** and **2** exhibit almost identical chemical shift pattern. Both 1:1 and 1:2 Mg:quinolone complexes are present in solution as suggested by the low solubility of **1** and **2**.

Acknowledgements

This work was supported by the Ministry of Higher Education, Science and Technology (MHEST), Republic of Slovenia, project P1-0175 and The Norwegian Research Council, Contract- 145183/V30. The crystallographic data were collected at the Institute for Mineralogy and Crystallography, Geocentre, University of Vienna (compound **1**) and in Ljubljana (compound **2**). P.D. is grateful to the MHEST, for funding through a junior researcher grant. Special thanks to Prof. B. Čeh and to Prof. J. Sletten for their help. This work is supported by COST Action D20.

Appendix A. Supplementary data

Supplementary material (**Figure S1**: ^{1}H NMR spectra of levofloxacin titrated with $MnCl_2$, **Table S1**: ^{1}H shifts for Mn(II) titration of levofloxacin and **Table S2**: Line widths for Mn(II) titration of levofloxacin) is available on request from the authors. CCDC-276067 (compound **1**) and CCDC-276068 (compound **2**) contain the supplementary crystallographic data for this paper. These data can be obtained free of charge at www.ccdc.cam.ac.uk/conts/retrieving.html [or from the Cambridge Crystallographic Data Centre, 12, Union Road, Cambridge CB2 1EZ, UK; fax: (internat) +44 1223/336 033; E-mail: deposit@ccdc.cam.ac.uk]. Supplementary data associated with this article can be found, in the online version, at doi:10.1016/j.jinorgbio.2006.06.011.

References

[1] K.E. Brighty, T.D. Gootz, in: V.T. Andriole (Ed.), The Quinolones, Academic Press, San Diego, 2000, pp. 33–97, and the references therein.
[2] L.A. Mitscher, P. Devasthale, R. Zavod, in: D.C. Hooper, J.S. Wolfson (Eds.), Quinolone Antimicrobial Agents, 2nd ed., American Society for Microbiology, Washington DC, 1993, pp. 3–53.
[3] L.-J. Ming, Med. Res. Rev. 23 (2003) 697–762, and the references therein.
[4] L.L. Shen, A.G. Pernet, Proc. Natl. Acad. Sci. USA 82 (1985) 307–311.
[5] I. Morrissey, K. Hoshino, K. Sato, A. Yoshida, I. Hayakawa, M.G. Bures, L.L. Shen, Antimicrob. Agents Chemother. 40 (1996) 1775–1784.
[6] H.J. Hwangbo, B.H. Yun, J.S. Cha, D.Y. Kwon, S.K. Kim, Eur. J. Pharm. Sci. 18 (2003) 197–203.
[7] I. Turel, Coord. Chem. Rev. 232 (2002) 27–47, and the references therein.
[8] B. Macias, M.V. Villa, I. Rubio, A. Castineiras, J. Borras, J. Inorg. Biochem. 84 (2001) 163–170.
[9] B. Macias, M.V. Villa, M. Sastre, A. Castineiras, J. Borras, J. Pharm. Sci. 91 (2002) 2416–2423.
[10] L.A. Mitscher, Chem. Rev. 105 (2005) 559–592.
[11] C. Sissi, M. Andreolli, V. Cecchetti, A. Fravolini, B. Gatto, M. Palumbo, Bioorg. Med. Chem. 6 (1998) 1555–1561.
[12] M. Palumbo, B. Gatto, G. Zagotto, G. Palu, Trends Microb. 6 (1993) 232–235.
[13] C.G. Noble, F.M. Barnard, A. Maxwell, Antimicrob. Agents Chemother. 47 (2003) 854–862.
[14] B. Llorente, F. Leclerc, R. Cedergren, Bioorg. Med. Chem. 4 (1996) 61–71.

[15] Y. Kwok, Q. Zeng, L.H. Hurley, J. Biol. Chem. 274 (1999) 17226–17235.
[16] I. Turel, I. Leban, M. Zupančič, P. Bukovec, K. Gruber, Acta Cryst. C 52 (1996) 2443–2445.
[17] T. Skauge, I. Turel, E. Sletten, Inorg. Chim. Acta 339 (2002) 239–247.
[18] P. Drevenšek, I. Turel, N. Poklar Ulrih, J. Inorg. Biochem. 96 (2003) 407–415.
[19] Z. Otwinowski, W. Minor, Methods Enzymol. 276 (1997) 307–326.
[20] G.M. Sheldrick, SHELX-97 Programs for Crystal Structure Analysis, University of Göttingen, Göttingen, Germany, 1998.
[21] G. Altiokka, Z. Atkosar, N.O. Can, J. Pharm. Biomed. Anal. 30 (2002) 881–885.
[22] I. Turel, A. Šonc, M. Zupančič, K. Sepčič, T. Turk, Metal Based Drugs 7 (2000) 101–104.
[23] P. Drevenšek, A. Golobič, I. Turel, N. Poklar, K. Sepčić, Acta Chim. Slov. 49 (2002) 857–870.
[24] I. Turel, A. Golobič, A. Klavžar, B. Pihlar, P. Buglyó, E. Tolis, D. Rehder, K. Sepčić, J. Inorg. Biochem. 95 (2003) 199–207.
[25] P. Drevenšek, T. Zupančič, B. Pihlar, R. Jerala, U. Kolitsch, A. Plaper, I. Turel, J. Inorg. Biochem. 99 (2005) 432–442.
[26] Y.X. Furet, J. Deshusses, J.C. Pechere, Antimicrob. Agents Chemother. 36 (1992) 2506–2511.
[27] A.G. Orpen, L. Brammer, F.H. Allen, O. Kennard, D.G. Watson, R. Taylor, J. Chem. Soc. Dalton Trans. (1989) S1–S83.
[28] F.H. Allen, O. Kennard, D.G. Watson, L. Brammer, A.G. Orpen, R. Taylor, J. Chem. Soc. Perkin Trans. II, 1987, S1-S19.
[29] Z.F. Chen, R.G. Xiong, J. Zhang, X.T. Chen, Z.L. Xue, X.Z. You, Inorg. Chem. 40 (2001) 4075–4077.
[30] Z.R. Qu, H. Zhao, L.X. Xing, X.S. Wang, Z.F. Chen, Z. Yu, R.G. Xiong, X.Z. You, Eur. J. Inorg. Chem. (2003) 2920–2923, and the references therein.
[31] K. Hoshino, K. Sato, K. Akahane, A. Yoshida, I. Hayakawa, M. Sato, T. Une, Y. Osada, Antimicrob. Agents Chemother. 35 (1991) 309–312.
[32] M. Sakai, H. Hara, S. Anjo, M. Nakamura, J. Pharm. Biomed. Anal. 18 (1999) 1057–1067.
[33] A. Mucci, L. Malmusi, M.A. Vandelli, M. Fresta, L. Schenetti, Med. Res. Chem. 6 (1996) 353–363.
[34] J. Shimada, K. Shiba, T. Oguma, H. Miwa, Y. Yoshimura, T. Nishikawa, Y. Okabayashi, T. Kitagawa, S. Yamamoto, Antimicrob. Agents Chemother. 36 (1992) 1219–1224.
[35] B.M. Sanchez, M.M. Cabarga, A.S. Navarro, A.D.G. Hurle, Int. J. Pharm. 106 (1994) 229–235.
[36] S. Lecomte, M.H. Baron, M.T. Chenon, C. Coupry, N.J. Moreau, Antimicrob. Agents Chemother. 38 (1994) 2810–2816, and the references therein.
[37] G. Navon, G. Valensin, in: H. Sigel (Ed.), Metal Ions in Biological Systems, vol. 21, Marcel Dekker, New York, 1987, pp. 1447–1453.
[38] E. Sletten, N.A. Froystein, in: H. Sigel (Ed.), Metal Ions in Biological Systems, vol. 32, Marcel Dekker, New York, 1996, pp. 397–418.
[39] I. Turel, J. Košmrlj, B. Andersen, E. Sletten, Metal Based Drugs 6 (1999) 1–4.
[40] S. Lecomte, M.T. Chenon, Int. J. Pharm. 139 (1996) 105–112.
[41] M. Sakai, A. Hara, S. Anjo, M. Nakamura, J. Pharm. Biomed. Anal. 18 (1999) 1057–1067.
[42] I.D. Blackburne, A.R. Katritzky, Y. Takenchi, Acc. Chem. Res. 9 (1975) 300–306.
[43] P.J. Crowley, M.J.T. Robinson, M.G. Ward, Tetrahedron 33 (1977) 915–925.
[44] A.R. Katritzky, R.C. Patel, F.G. Riddell, Angew. Chem. Int. Ed. Engl. 20 (1981) 521–529.
[45] P. Ball, In: V.T. Andriole (Eds.), The Quinolones, Academic Press, San Diego, 2000, pp. 1–31.
[46] R. Stahlmann, H. Lode, V.T. Andriole (Eds.), The Quinolones, Academic Press, San Diego, 2000, pp. 397–453.
[47] I. Turel, I. Leban, G. Klintschar, N. Bukovec, S. Zalar, J. Inorg. Biochem 66 (1997) 77–82.
[48] I. Turel, L. Golič, P. Bukovec, M. Gubina, J. Inorg. Biochem. 71 (1998) 53–60.
[49] G. Palu, S. Valisena, G. Ciarocchi, B. Gatto, M. Palumbo, Proc. Natl. Acad. Sci. USA 89 (1992) 9671–9675.
[50] C. Sissi, E. Perdona, E. Domenici, A. Feriani, A.J. Howells, A. Maxwell, M. Palumbo, J. Mol. Biol. 31 (2001) 195–203.
[51] C.J.R. Willmott, A. Maxwell, Antimicrob. Agents Chemother. 37 (1993) 126–127.
[52] M.-H. Hou, H. Robinson, Y.-G. Gao, A.H.-J. Wang, Nucleic Acids Res. 32 (2004) 2214–2222.